Photodiagnosis and Photodynamic Therapy 27 (2019) 7–18

Contents lists available at ScienceDirect

Photodiagnosis and Photodynamic Therapy

journal homepage: www.elsevier.com/locate/pdpdt

Enhancing osteoblast functions on biofilm-contaminated titanium alloy by concentration-dependent use of methylene blue-mediated antimicrobial photodynamic therapy

Tsun-Chin Huang[a], Chun-Ju Chen[a], Chun-Cheng Chen[b,c,**], Shinn-Jyh Ding[a,b,*]

[a] Institute of Oral Science, Chung Shan Medical University, Taichung City 402, Taiwan
[b] Department of Stomatology, Chung Shan Medical University Hospital, Taichung City 402, Taiwan
[c] School of Dentistry, Chung Shan Medical University, Taichung City 402, Taiwan

ARTICLE INFO

Keywords:
Dental implant
Peri-implantitis
Photodynamic therapy
Antimicrobial efficacy
Osteogenic activity
Antimicrobial photodynamic therapy

ABSTRACT

The concentration of methylene blue (MB) photosensitizer could affect the eradication efficacy of antimicrobial photodynamic therapy (aPDT) in the treatment of contaminated implants, which is linked to the osseointegration of the implant. We evaluated osteoblast functions on the contaminated SLA (sandblasting, large-grit and acid-etching) Ti alloy surfaces after the concentration-dependent use of MB-aPDT. Totally 1164 SLA discs were randomly distributed for the analyses of antibacterial efficacy and osteoblast functions. Gram-negative (*Aggregatibacter actinomycetemcomitans; A. actinomycetemcomitans*) or Gram-positive (*Streptococcus mutans; S. mutans*) adhered on disc samples was subjected to aPDT with different MB concentrations (200, 250, 300, 350, and 400 μg/mL) using 660 nm diode laser with maximum output 80 mW for 1 min irradiation (4.8 J/cm^2). Bactericidal effect was examined by viability, morphology, and lipopolysaccharide (LPS) assays. The disinfected disc surfaces by MB-aPDT to support osteoblast-like MG63 attachment, proliferation, differentiation, and mineralization were assessed for the predetermined culture time intervals. The statistical differences between the means were performed using a one-way analysis of variance (ANOVA) with a *post hoc* Scheffe test. The results of the morphology observation and bacterial survival examination consistently indicated a remarkably lower quantity of bacterial colonies on biofilm-contaminated surfaces after the aPDT treatment with higher MB concentration. Similarly, the higher MB concentration in aPDT resulted in the lower LPS amounts remaining on the *A. actinomycetemcomitans*-contaminated surfaces. Intriguingly, the expression of osteoblast cultured on disinfected surfaces using aPDT with higher MB concentration was comparable to the control without contamination. Within the limits of this in vitro model, this formulation of 400 μg/mL MB used in aPDT may be not only the lethal concentration against the 2 bacteria-contaminated implants, but it could also enhance the osteoblast functions on the contaminated implants. Nevertheless, the efficacy in the clinical practice for peri-implantitis therapy remains to be studied.

1. Introduction

Peri-implantitis is defined as an inflammatory lesion of peri-implant tissues due to microbial plaque accumulation and bacterial infections, which could result in loss of supporting bone [1]. Elimination of the causative bacteria and peri-implant pockets around the contaminated implant surface is crucial to treat the peri-implantitis, which in turn stimulates re-osseointegration [1–3]. Current therapy techniques in the peri-implantitis treatment involve either periodic mechanical debridement of microbial biofilms or maintaining therapeutic concentrations of antimicrobials, both of which are limited [4–6]. For example, mechanical debridement using air-powder abrasive system would damage the implant surfaces [6]. Commonly used antimicrobials such as sodium hypochlorite and chlorhexidine are effective at killing microorganisms but not completely removing biofilm on titanium implants [7,8]. Mechanical debridement alone or combined with chlorhexidine antiseptics fails to effectively remove the bacterial LPS, which would foster a lower numbers of adhered osteoblast cells on the disinfected sample compared with those cultured on the uncontaminated sample [9]. Systemic or topical antibiotics are also considered as adjuncts to mechanical

* Corresponding author at: Institute of Oral Science, Chung Shan Medical University, Taichung City 402, Taiwan.
** Corresponding author at: School of Dentistry, Chung Shan Medical University, Taichung City 402, Taiwan.
E-mail addresses: fw3256@gmail.com (C.-C. Chen), sjding@csmu.edu.tw (S.-J. Ding).

https://doi.org/10.1016/j.pdpdt.2019.05.021
Received 8 February 2019; Received in revised form 7 April 2019; Accepted 17 May 2019
Available online 19 May 2019
1572-1000/

debridement in the management of peri-implantitis. However, the use of antibiotics does not effectively eliminate bacterial colonization on the surface of implants, which possibly forms antibiotic resistant biofilm [10,11]. In a word, LPS-induced inhibition of osteogenesis might be due to the inhibition of the osteoblast differentiation and mineralization [12]. Removal of LPS is a great challenge that needs to be overcome. Therefore, the development of alternative antimicrobial modalities is of importance.

The non-invasive aPDT to control biofilm growth has attracted much interest. The antimicrobial efficacy of aPDT is based on the accumulation of the photosensitizers, such as MB and toluidine blue O (TBO), to a significant extent in or at the cytoplasmic membrane [13]. After absorption of light from the low power laser with appropriate wavelength, the photosensitizer is converted to triplet excited state, which in turn causes either the formation of radical (type I) or singlet oxygen (type II) species [13,14]. These highly reactive oxygen species (ROS) initiate further oxidative reactions in the proximate environment, such as the bacterial cell wall, lipid membranes, enzymes, or nucleic acids, to induce the irreversible damage in bacteria [12,13]. In fact, the aPDT treatment has emerged as an adjunct to mechanical debridement for peri-implantitis to reduce bacteria and LPS adherent to titanium implant surface without causing damage to surface microstructure [15,16]. The combined use of mechanical debridement (e.g. titanium brush) and MB-aPDT is more efficient in reducing the number of *Staphylococcus aureus* in both polished and rough titanium surfaces than mechanical debridement alone and MB-aPDT alone [17]. Randomized controlled clinical trials in patients with peri-implantitis suggest that the use of aPDT with mechanical debridement can definitely result in significant reduction in the level of attachment scores compared with other interventions examined [18]. However, aPDT can also be used as an alternative to conventional therapy rather than an adjunct. For example, Marotti and the colleagues [5] used 100 μg/mL MB-aPDT with light energy of 12 J in the decontamination treatment of anodized implants, which its efficacy was comparable to the chlorhexidine.

It is well-known that bacterial adhesion and biofilm growth adversely affects the osseointegration on implant surface [19]. Undoubtedly, a successful treatment may reside in the high extent of bacterial removal. Moreover, the subsequent effect of residual biofilm on the osseointegration of disinfected implants requires further investigation [20,21]. The osseointegration of the implant plays an important role in evaluating implant success. Different results of biocompatibility on the surface of disinfected implants are found using various treatment modalities [22,23]. Chellini et al. [22] analyzed the responses of osteoblast-like Saos2 cells and adult human bone marrow-mesenchymal stromal cells to oxidized titanium surfaces pre-treated with a GaAlAs diode laser eradicating bacteria. Their results indicated the diode laser irradiation preserved the biocompatibility of the titanium surface. However, Schwarz et al. found that Er:YAG laser, an ultrasonic system, plastic curettes, and chlorhexidine failed to restore the biocompatibility of previously-contaminated SLA titanium surfaces [23]. To this end, the osteoblast functions incubated on the surfaces of disinfected samples using aPDT should be examined to understand the effect of aPDT on osseointegration, which can also clarify the LPS-induced inhibition of osteogenesis. To the best of our knowledge, there was no report about the influence of the biofilm-contaminated titanium surfaces following MB-aPDT on osteogenesis. This work was the first to evaluate the osteoblast attachment, proliferation, differentiation, and mineralization responses to the disinfected surfaces treated by the use of MB-aPDT.

Methylene blue (MB) has been widely used as a photosensitizer in aPDT for its high quantum yield of singlet oxygen ($^1O_2$) generation [14]. Very recently, we reported that MB-aPDT could effectively eliminate biofilm-associated bacterial populations on SLA-modified titanium alloy surfaces using a 200 μg/mL MB for 1 min of irradiation time [16]. However, there was residual biofilm on SLA-modified surfaces. According to the literature [24,25], it is difficult to completely clean a well-established biofilm on the implant surfaces. More effective eradication of bacteria might be achieved by means of the increase in MB concentration in aPDT. For this reason, in this work the higher MB concentration (200, 250, 300, 350, and 400 μg/mL) than those in previously used concentrations at pH 7 for 1 min of aPDT treatment was utilised. It was hypothesized that the higher MB concentration was more effective at eradicating biofilm-contaminated SLA Ti alloy surfaces, which promoted osteoblast functions on the disinfected surfaces comparable to the uncontaminated surfaces. Therefore, the bactericidal efficacy and osteogenic activity of the concentration-dependent MB-aPDT on contaminated surfaces were investigated.

2. Material and methods

2.1. Preparation of titanium alloy

Commercially available 3 mm-thick Ti-6Al-4 V alloys (ASTM F136-84; Titanium Industries, Parsippany, NJ, USA) of 10 × 10 mm^2 were selected as the substrate materials. A total of 1164 Ti alloy discs were wet-ground with a 1200-grit SiC abrasive paper (3 M Wetordry TriMite 734, St. Paul, MN, USA), followed by sandblasting with Al_2O_3 particles with 100 μm (Korox, Bego, Bremen, Germany) for 10 s. The air-pressure was 3.5 bar using a Taicrown P-002B machine (Taichung, Taiwan) and the distance between the orifice and the metal surface was approximately 10 mm [16]. Afterwards, the discs were subjected to by acid etching in $HCl/H_2SO_4/H_2O$ (1:1:100) at 100 °C for 30 min to obtain SLA surface [8]. The SLA discs were then ultrasonically cleaned in acetone and ethanol for 20 min at each step, rinsed in deionized water, and then dried in an oven at 60 °C. Ti alloy discs were randomly allocated to 24-well culture plates and then sterilized by soaking in a 75% ethanol solution and exposure to UV light overnight [26].

2.2. Bacteria culture

Gram-negative *A. actinomycetemcomitans* (IDH 781) and Gram-positive *S. mutans* (ATCC 700610) bacteria were used. The bacteria from an isolated single colony were inoculated into Wilkins-Chalgren Anaerobe broth (Oxoid, Hampshire, UK) and cultured in incubator for 24 h at 37 °C, which the optical density of about 1.0 was achieved at 600 nm using a Beckman Coulter DU-640 spectrophotometer (Beckman Instruments, Fullerton, CA). Bacteria solutions were diluted by Wilkins-Chalgren Anaerobe broth to a density of 2 × 10^6 CFU/mL for seeding.

2.3. Bacterial adhesion

For bacterial adhesion, 1 mL of bacteria suspensions per well in 24-well culture plates was seeded onto the sterilized Ti alloy surfaces under anaerobic conditions at 37 °C for 24 h [16]. The contaminated discs were washed two times with phosphate buffer solution (PBS) for following photodynamic treatment. The experimental procedure including MB-aPDT, antibacterial analyses, and cell function assay was illustrated in Fig. 1.

2.4. Preparation of methylene blue

Methylene blue ($C_{16}H_{18}ClN_3S$; Riedel-deHaen Co, Buffalo, NY, USA) powder was used without further purification. The appropriate amount of MB powder was dissolved in PBS at pH 7 by shaking. The five concentrations of 200, 250, 300, 350, and 400 μg/mL MB solutions were separately prepared and stored in the dark at 4 °C for usage later.

2.5. Photodynamic treatment

After culture for 24 h on 24-well culture plates, the contaminated samples were sprayed with 100 μL of MB for 1 min of reaction and then washed by PBS. After which, the samples were irradiated with a low

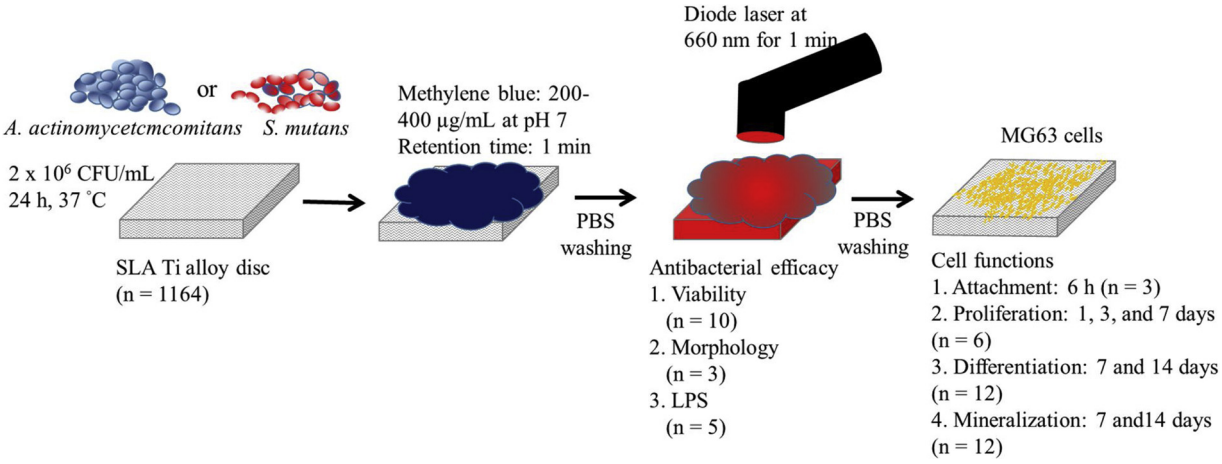

Fig. 1. Schematic illustration of the course of experiments.

level AlGaInP diode laser (Aculas-HB, Konftec, New Taipei City, Taiwan) with maximum output 80 mW working at 660 nm for 1 min, which corresponded to fluency of 4.8 J/cm^2 [16]. The laser beam from the rod end with an output diameter of 8 mm was irradiated focusing onto the substrate in continuous mode. The distance between the irradiated sample and the laser tip with 1 cm diameter was 10 mm at an incidence angle of 90 ˚.

2.6. Bacterial viability

The antimicrobial efficacy of MB-aPDT against bacterial species was determined using an alamarBlue (Invitrogen, Grand Island, NY, USA) assay that was used for real-time and repeated monitoring of bacterial viability. The number of viable bacteria can be estimated via redox reactions between the fluorometric/colorimetric growth indicator dye of alamarBlue and metabolically active bacteria [16]. After the end of the laser treatment, 600 μL of solution at a ratio of 1:10 of alamarBlue to broth was added to 24-well culture plates, followed by being incubated at 37 ˚C for 20 min. Subsequently, 100 μL of the solution in each well was transferred to a new 96-well tissue culture plate. Plates were read in a Sunrise Microtiter reader (Tecan Austria Gesellschaft, Salzburg, Austria) at 570 nm with a reference wavelength of 600 nm. The contaminated Ti alloy discs without treatment were used as a control, while the five different concentrations of MB alone and MB-aPDT groups were assigned to the experimental groups. The changes in the antimicrobial effectiveness of different concentrations of MB solutions before and after laser treatments against bacterial species were expressed as the reduction percentage normalized to that of the control by means of the absorbance change [27]. The absorbance value was proportional to the number of viable bacteria. The reduction percentage (%) was calculated as follows: (absorbance of alamarBlue obtained on the control-absorbance of alamarBlue obtained on treated samples)/absorbance of alamarBlue obtained on the control) × 100%. The data provided for each group were the mean of ten independent measurements.

2.7. Morphology observation

To observe surface morphology on the contaminated Ti alloy surfaces, the bacterial-contaminated group was used as the control. The disinfected groups using MB alone or MB-aPDT were examined, and three specimens per group were washed three times with PBS and fixed in 2% glutaraldehyde (Sigma, St. Louis, MO, USA) [16]. The specimens were then dehydrated using a graded ethanol series for 20 min at each concentration. The dried specimens were mounted on stubs, coated with gold layer, and viewed using scanning electron microscopy (SEM; JEOL JSM-7800 F, Tokyo, Japan).

2.8. LPS detection

After MB-aPDT, the LPS amounts remaining on the titanium alloy surfaces were quantified using a ToxinSensor chromogenic Limulus Amebocyte Lysate endotoxin assay kit (GenScript, Piscataway, NJ, USA) according to the manufacturer's instructions [16]. The contaminated Ti alloy substrate without MB-aPDT treatment was regarded as a control. Five replicates were carried out for each group, and the results were expressed in terms of absorbance at 545 nm.

2.9. MG63 cell culture

To examine the effect of MB-aPDT on cell functions of the decontaminated Ti alloy discs, MG63 human osteoblast-like cells (BCRC 60279; Hsinchu, Taiwan) were used. The cells were suspended in Dulbecco's modified Eagle medium (DMEM; Gibco, Langley, OK) containing 10% fetal bovine serum (FBS) (Gibco) and 1% penicillin (10,000 U/mL)/streptomycin (10,000 μg/mL) solution (Gibco) in 5% CO_2 at 37 ˚C [26]. MG63 cell suspensions at a density of 10^4 cells per well were seeded over each of the samples. MG63 cells cultured on uncontaminated Ti alloy samples were used as a control. There were five experimental groups consisting of *A. actinomycetemcomitans*-contaminated or *S. mutans*-contaminated surfaces treated by different concentration uses of MB-aPDT.

2.10. Cell attachment

To observe cell attachment, the cells were washed three times with PBS and fixed in 2% glutaraldehyde (Wako, Tokyo, Japan) at 4 ˚C for 2 h after 6 h of incubation. After dehydration in a graded ethanol series for 20 min at each concentration and drying overnight, the cells were coated with a gold layer and observed under a SEM. Three samples were used for each group.

2.11. Cell proliferation

After 1, 3, and 7 days of incubation, cell proliferation was examined using the MTT (3-(4,5-dimethylthiazol-2-yl)-2,5-diphenyltetrazolium bromide; Sigma–Aldrich) assay, in which tetrazolium salt is reduced to formazan crystals by the mitochondrial dehydrogenase of living cells [27]. Briefly, 4 h before the end of the incubation period, 200 μL of 0.5 mg/mL MTT solution in DMEM containing 1% penicillin/streptomycin and 200 μL of dimethylsulfoxide (DMSO; Sigma–Aldrich) were added to each well. The plates were then shaken until the formazan

crystals had dissolved, and 100 μL of the solution from each well was transferred to a 96-well tissue-culture plate. Plates were read in a Sunrise microplate reader at 570 nm with a reference wavelength of 650 nm. The results were obtained in six independent measurements and reported in terms of absorbance.

2.12. Alkaline phosphatase activity

To evaluate the early cell differentiation, the alkaline phosphatase (ALP) activity assay was carried out using a TRACP & ALP assay kit (Takara, Shiga, Japan) according to the manufacture's instructions [27]. ALP catalyzes the hydrolysis of the colorless organic phosphate ester substrate, p-nitrophenyl phosphate (pNPP), to p-nitrophenol, a yellow product, and phosphate. To perform the assay, after 7 and 14 days of incubation, the cells were washed with physiological saline (150 mM NaCl) and lysed in 50 μL of lysis buffer (1% NP40 in 150 mM NaCl). For measurement purposes, 50 μL of the substrate solution (20 mM Tris–HCl, 1 mM $MgCl_2$, 12.5 mM pNPP, pH = 9.5) was added to each well and allowed to react at 37 °C for 30 min in the dark. The reaction was stopped by the addition of 50 μL of 0.9 M NaOH and read at 405 nm using a Sunrise microplate reader. Data were the mean of twelve independent measurements.

2.13. Calcium quantification

The mineralized matrix synthesis was analyzed using an Alizarin Red S staining method, which identifies calcium deposits. After culture for 7 and 14 days, the cells were washed with PBS and fixed in 4% paraformaldehyde (Sigma–Aldrich) for 10 min at 4 °C. This was followed by staining for 10 min in 0.5% Alizarin Red S (Sigma–Aldrich) in PBS at room temperature. Cells were completely washed with PBS and then observed using an optical microscope (BH2-UMA; Olympus, Tokyo, Japan). To quantify matrix mineralization, the calcium mineral precipitate was destained by 10% cetylpyridinium chloride (Sigma–Aldrich) in PBS for 30 min at room temperature [27]. The absorbance of Alizarin Red S extracts was measured at 562 nm using a Sunrise microplate reader. Mean absorbance values were obtained from twelve independent experiments.

2.14. Statistical analysis

All the results are expressed as the mean ± standard derivation for the total number of replicate experiments indicated unless otherwise stated. ANOVA was used to evaluate significant differences between the means for the intragroup comparison including the reduction percentage of bacterial viability, LPS, cell proliferation, differentiation, and calcium deposit in the *A. actinomycetemcomitans*-contaminated or *S. mutans*-contaminated groups. The intergroup comparison of bacterial viability between MB alone and MB-aPDT was also performed by ANOVA. Statistical analysis was performed with the SPSS 14.0 software for Windows (SPSS Inc, Chicago, IL, USA). Scheffe's multiple comparisons were used to determine the significance of the standard deviations between the sample measurements for each bacterial-contaminated intragroup. The result was considered statistically significant when the *p*-value was less than 0.05.

3. Results

3.1. Bacterial viability

The changes in the reduction percentage of (a) *A. actinomycetemcomitans* and (b) *S. mutans* seeded on the Ti alloy surfaces after treatment by MB alone or MB-aPDT as a function of MB concentrations are shown in Fig. 2, which the significant difference ($p < 0.05$) from the 200 μg/mL group for the intragroup comparison was presented. Before aPDT treatment, the decontamination efficacy of MB alone against the two bacterial species increased with the increasing MB concentrations, which indicated statistical differences ($p < 0.05$). The 200 μg/mL MB alone eliminated the number of 40% *A. actinomycetemcomitans* (Fig. 2a) and 32% *S. mutans* (Fig. 2b), whereas the highest MB concentration (400 μg/mL) killed remarkably 62% of the viable *A. actinomycetemcomitans* and 71% of the viable *S. mutans*. After MB-aPDT, as expected, significantly ($p < 0.05$) greater reduction percentage was found when compared with corresponding group treated with MB alone. Unsurprisingly, aPDT with higher MB concentration effectively killed the bacteria than obtained by using the lower concentration. Of note, the reduction percentage of bacterial counts could achieve more than 85% for all concentration use of MB-aPDT, in particular, the MB concentration more than 300 μg/mL resulted in the 100% reduction.

3.2. Bacterial adhesion

To attest the effective elimination effect of MB-aPDT on the contaminated surfaces, the bacterial colonies on the Ti alloy surfaces was observed by SEM. Fig. 3 shows that after seeding bacterial species for 24 h on the SLA surfaces, it can be clearly seen that the two bacteria uniformly adhered to the surfaces. Both Gram-negative bacteria *A. actinomycetemcomitans* and Gram-positive bacteria *S. mutans* presented a short rod-shaped morphology. When the biofilm-contaminated samples were treated with MB alone, it seems that bacterial counts of colonies on the Ti alloy surfaces were decreased with an increase in the MB concentration. By contrast, the various MB-aPDT treatments remarkably reduced the number of bacterial CFU (Fig. 4) when compared with the corresponding group with MB alone. As expected, relatively few amounts of bacteria were observed on 400 μg/mL MB-aPDT samples.

3.3. Residual LPS level

To further reveal the effectiveness of MB-aPDT treatment as a function of MB concentration, the amounts of residual LPS from *A. actinomycetcmcomitans* on the decontaminated Ti alloy surfaces were examined. Fig. 5 shows an apparently high LPS level in the control without MB-aPDT treatment. Contrary to the finding, the LPS amounts remained on the MB-aPDT-treated surfaces were significantly ($p < 0.05$) reduced. More importantly, with the increasing MB concentration the residual LPS amounts diminished. There was a significant ($p < 0.05$) difference between 200 μg/mL and 350 μg/mL (or 400μg/mL) MB-aPDT.

3.4. Cell attachment

The initial cell attachment on disinfected implant surfaces was examined after 6 h of culture, as shown in Fig. 6. The cells attached to the uncontaminated surfaces were flat with an intact, well-defined morphology, indicating the good survival of MG63 cells (Fig. 6a). Interestingly, the cells cultured on the *A. actinomycetcmcomitans*-decontaminated surface were also spread out, similar to that on the uncontaminated surface, although it was possible to observe a few *A. actinomycetcmcomitans* bacteria (Fig. 6b–f). Similarly, Fig. 7 shows the MG63 cells attached well on the *S. mutants*-decontaminated surface, indicating the abundant stress fibers. It seems that cell attachment was not adversely affected in the presence of few microorganisms.

3.5. Cell proliferation

Fig. 8 indicates that the absorbance steadily increased on day 1 through day 7 when the cells were cultured on the disinfected surfaces using various MB-aPDT treatments, demonstrating the increasing number of viable cells. At first glance the data pointed out a prominent trend, which the MB-aPDT treatment with a higher MB concentration presented significantly ($p < 0.05$) higher cell proliferation than those

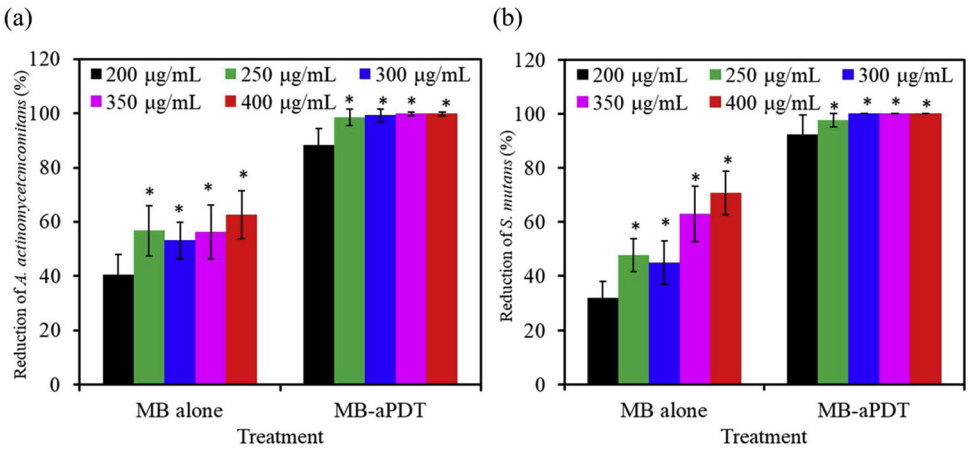

Fig. 2. The reduction percentage of (a) *A. actinomycetemcomitans*-contaminated or (b) *S. mutans*-contaminated samples subjected to MB alone and MB-aPDT treatments. An asterisk (*) shows the significant difference ($p < 0.05$) from the 200 μg/mL group.

with a lower MB concentration after all culture time intervals on the two different biofilm-contaminated samples. Of note, the 350 and 400 μg/mL groups gave rise to higher values in the cell proliferation of MG63 than the other MB-aPDT groups, which was comparable to the control ($p > 0.05$). For example, on day 7, the 400 μg/mL MB-aPDT against *A. actinomycetcmcomitans*- and *S. mutants*-contaminated samples had absorbance ratios of 97% and 101% referenced to the uncontaminated control, respectively.

3.6. ALP activity

Fig. 9 shows the results of the intracellular ALP level for assaying the early osteoblastic differentiation after 7-day and 14-day cultures. A significantly lower ALP level was measured for 200 and 250 μg/mL groups in comparison with the other concentration groups at all culture time points. The aPDT treatment with higher MB concentration such as 350 and 400 μg/mL produced a higher ALP level, which was very close to those obtained in the control.

3.7. Mineralization

The ability of cells to produce mineralized matrix is important with respect to occurrence of re-osseointegration for the disinfected implant. Alizarin Red S staining is a common histochemical technique used to detect calcium deposits in mineralized tissues and cell cultures. Fig. 10 shows the increased amount of mineralization over time. The cells grown on the Ti control surfaces and *A. actinomycetcmcomitans*-disinfected surfaces treated by the 400 μg/mL MB-aPDT after culture for 7 and 14 days presented a comparable content of calcium deposits, which were no significant differences ($p > 0.05$) (Fig. 10a). In contrast, the 200–300 μg/mL MB-aPDT groups resulted in a significantly ($p < 0.05$) lower mineralization than the Ti control. Similar results were revealed in the MG63 cell cultured to *S. mutants*-disinfected surface (Fig. 10b), and the enhanced effect of 400 μg/mL MB on mineralization was more than those of the other concentrations.

4. Discussion

A variety of decontamination methods in the peri-implantitis treatment include mechanical debridement, the use of antimicrobial agent, laser irradiation, and aPDT. Regarding the laser application, the commonly used lasers for peri-implant treatment include CO_2, diode, and Er:YAG (erbium-doped yttrium aluminium garnet) lasers because of their hemostatic properties, selective calculus ablation, and bactericidal effects [5,28,29]. However, an undesired increase in temperature during the action of a high power laser may result in tissue damage, such as bone resorption and pulp tissue lesions [30]. In contrast to the high power laser, low-level laser therapy (LLLT) (also known as photobiomodulation (PBM) or cold (soft) laser therapy) is a non-pharmaceutical, non-thermal and non-invasive clinical treatment, which produces analgesic, anti-inflammatory, and biostimulative effects on the healing and regeneration of hard and soft tissues [31–34]. Hübler et al. [32] reported that LLLT had a positive effect on the biomodulation of newly formed bone at the site of distraction osteogenesis. The underlying mechanism of LLLT with biostimulation at the cellular level may be that laser energy is absorbed by intracellular chromophores, which is converted to metabolic energy and then used by the mitochondrial respiratory chain to produce ATP and facilitate DNA activity as well as RNA and protein synthesis [35,36]. Compared to LLLT, another phototherapy modality is aPDT that combines LLLT with a photosensitizer binding to target microorganisms. aPDT can be used alone or as an adjunct to conventional mechanical debridement. In addition to bactericidal efficacy, aPDT also contributes to the periodontal repair processes by inhibiting the bone resorption and stimulating cell proliferation in ovariectomized rats with induced periodontal disease [37]. Almeida et al. [38] found that the bactericidal effect of MB-aPDT reduced bone loss in periodontitis induced by the ligature in the furcation region compared with the LLLT group.

Successful dental implant treatment requires adequate osseointegration that is dependent on osteogenesis of osteoblasts around the implant, but the prevention of bacterial infection is also a critical factor in the success of a long-term implantation [39]. It is imperative for developing novel approaches for biofilm removal of implant surfaces, which subsequently favors cell adhesion and growth [9,40]. Following an earlier study, we further compared the antibacterial efficacy of the MB concentrations ranging from 200 to 400 μg/mL MB at pH 7 during aPDT against two different bacterial species. It is worth noting that from the viewpoint of the clinical practice, the choice of solution pH at 7 should also be considered, although the alkaline pH of MB medium is not only beneficial to the quantum yield of $^1O_2$ generated by MB [41], but also the photolysis rate [42]. The previous study also elucidates that the alkaline pH solution (pH 10) gives rise to a significantly lower residual LPS amount than those obtained from the corresponding groups at the neutral pH solution [16]. Nevertheless, Leblebicioglu et al. [43] demonstrated impaired chemotaxis at pH 7.7 and 8.2, but no change was observed at pH 6.7. Lardner [44] reported that increasing the pH of the medium above 7.6 resulted in a significant decrease in cell movement, with complete and irreversible inhibition of leukocyte motility occurring at pH 7.9. It can therefore be speculated that excessive abnormal pH (high alkaline) might damage the host tissue surrounding the implants. Regarding the bacterial species, gram-positive *S. mutans* is an important bacterial stain in the initiation of dental caries, whereas

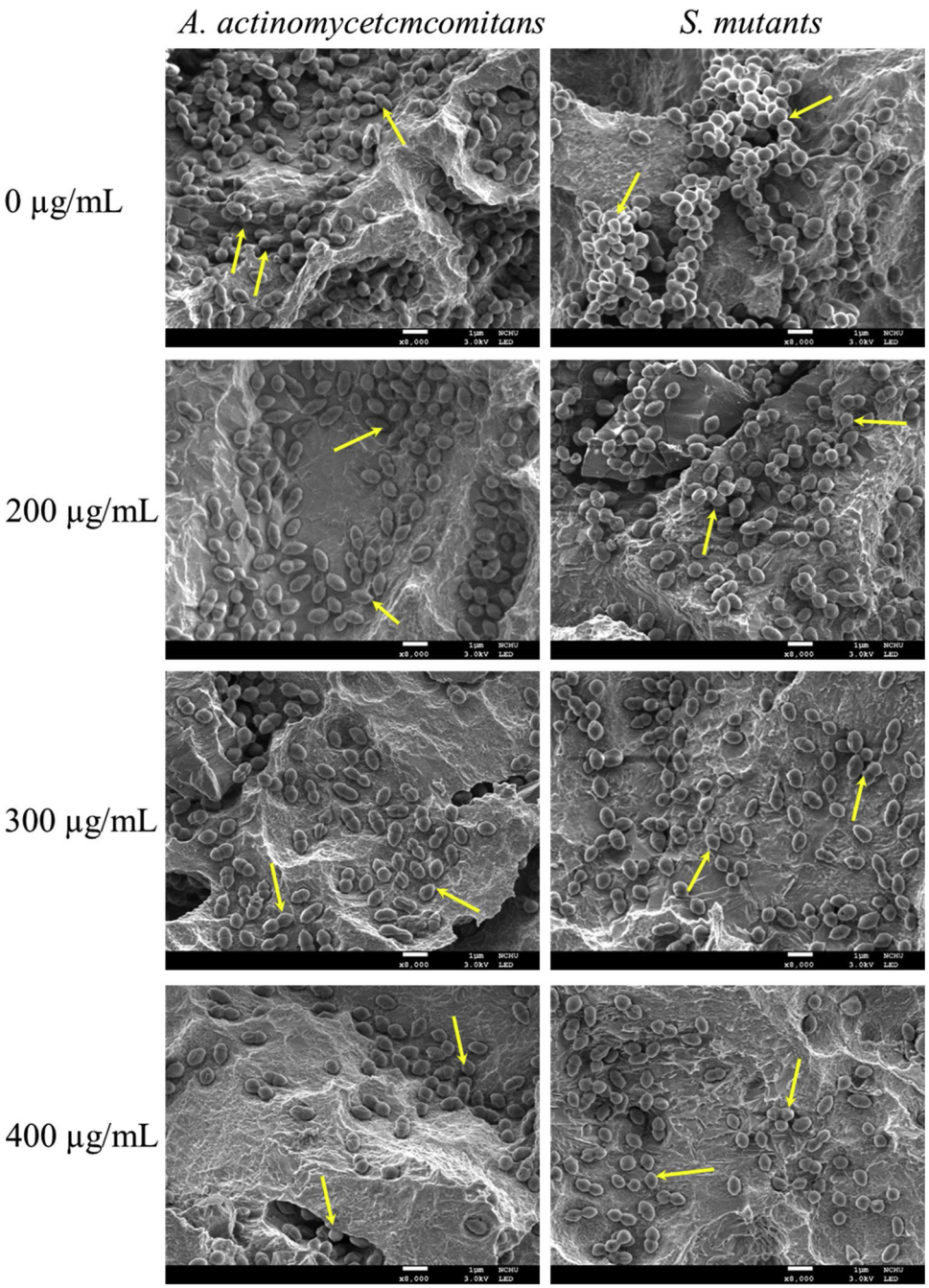

Fig. 3. SEM images of the *A. actinomycetcmcomitans*-contaminated or *S. mutants*-contaminated surfaces after treatment with different MB concentrations alone. The arrows indicated the presence of bacteria.

Gram-negative *A. actinomycetemcomitans* microaerophilic bacteria are one of the causative agents of periodontal disease. Particularly, the enhanced effect of various MB-aPDT treatments on osteoblast functions cultured on the disinfected SLA implant surfaces was focused. Due to high surface micro-roughness of the SLA implants, the SLA process has been widely utilised to treat titanium implants for improving the osseointegration [45]. Therefore, in this study the SLA disc samples were used to simulate the commonly used implant surfaces.

Biofilm synthesis takes place via a number of well-organized processes including initial adhesion, the formation of three-dimensional structures, and the development of mature biofilm [46]. It necessitates examining the adhesion count and residual LPS of bacterial colonization on the SLA surfaces before and after aPDT. In this study, the exposure of the Ti alloy samples to the bacterial suspension induced obvious bacterial colonization as assayed by SEM images and LPS levels after the culture for 24 h. An alamarBlue assay was used to examine bacterial survival on the sample surfaces. The alamarBlue method represents a high throughput assay alternative to the classic type of colony-forming units (CFU) assay [47]. Given that cationic MB photosensitizer can target bacterial membranes of both Gram-positive and Gram-negative bacteria by virtue of interaction with anionic regions from bacterial cell walls [20], it diminishes bacterial growth [48]. Indeed, the MB alone revealed concentration-dependent bactericidal activity against clinically relevant microorganisms because of the concentration-dependent ROS production [49]. Usacheva et al. [51] observed that the numbers of bacteria killed with MB or TBO alone increased with increasing dye concentrations in the range of 25–375 μM. However, it showed no signs of effective eradication

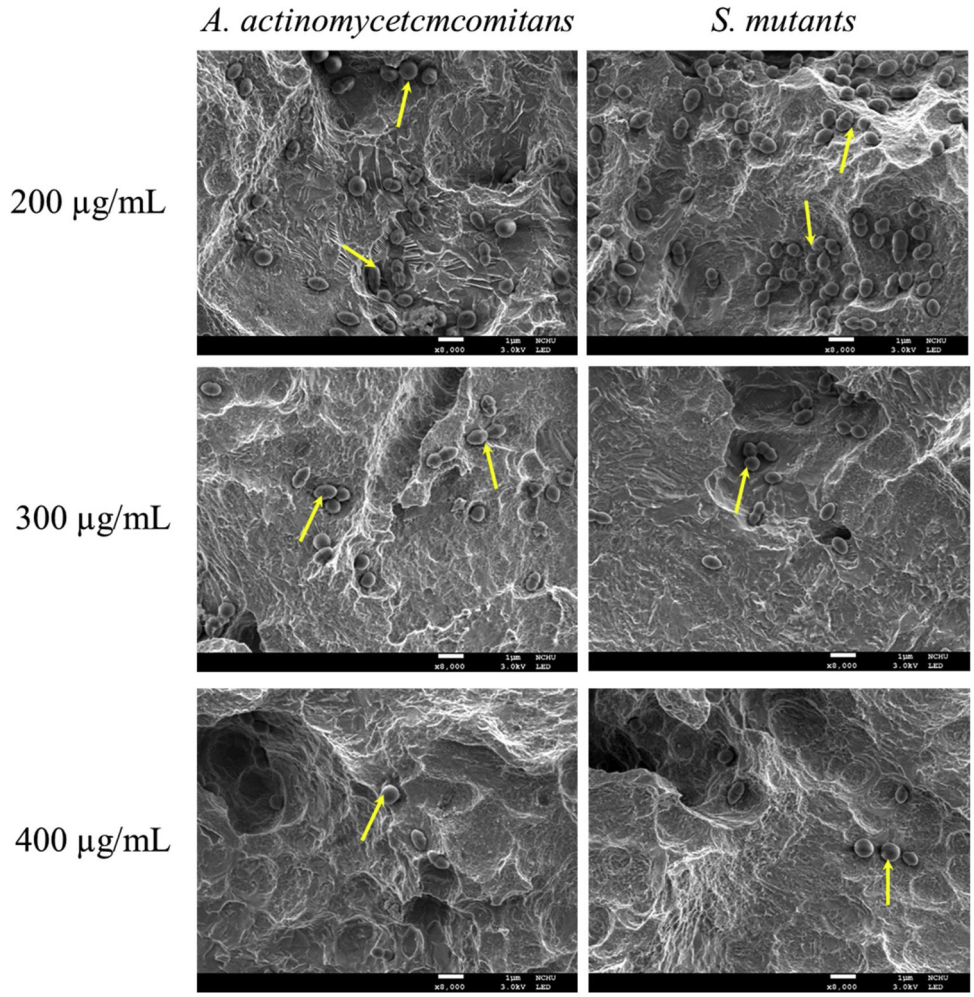

Fig. 4. SEM images of the *A. actinomycetcmcomitans*-contaminated or *S. mutants*-contaminated surfaces after treatment with different MB concentrations in aPDT. The arrows indicated the presence of bacteria.

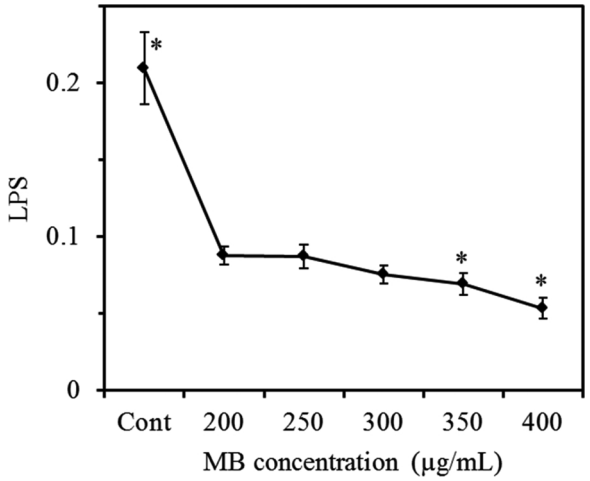

Fig. 5. Residual lipopolysaccharide (LPS) levels from *A. actinomycetcmcomitans* on contaminated surfaces before and after various MB-aPDT treatments. The contaminated Ti alloy without aPDT was used as a control. An asterisk (*) shows the significant difference ($p < 0.05$) from the 200 μg/mL group.

effectiveness from the results of alamarBlue method. The findings were consistent with a previous study reported by Fontana et al. [51], which the percentage survival of bacteria was assayed using the CFU assay.

To more effectively eliminate the bacteria, MB-aPDT was used in place of the MB alone. As a result, the reduction percentages of the two viable bacteria were obviously enhanced in MB-aPDT in comparison with the MB alone. Of note, higher MB concentrations in the MB-aPDT procedure led to greater bactericidal effectiveness than the lower MB concentrations, which was in line with the previous studies [16,51]. In addition, the SEM images supported the results of the survival assay. Contrary to the findings, Aureliano et al. [49] elucidated that the use of the lower MB concentration in antiparasitic photodynamic therapy induced the higher leishmanicidal effect. They assumed that high MB concentrations resulted in an optical shielding that could avoid the light penetration through the microorganism suspension and form high dimer/monomer ratio due to metachromasy effect. Differences in the concentration-dependent analysis results with regard to MB-aPDT could be possibly because of different evaluation methodology [5], photosensitizer concentration [50], and laser parameters [52].

In addition to the inactivation of pathogenic bacteria, it is important to eliminate cytotoxic cell components as endo- and exotoxins from implant surfaces [28]. LPS, also termed endotoxin, is the major cell wall component of Gram-negative bacteria, such as *A. actinomycetemcomitans*. LPS remaining on the titanium alloy surfaces would facilitate subsequent microbial adhesion [53]. On the other hand, the residual LPS adversely affects cellular metabolism and reduces the proliferation rate of connective tissue cells [28]. Although both bacterial survival assay and morphology observation consistently revealed the superior decontamination efficacy of MB-aPDT on the biofilm-contaminated Ti alloy surfaces in this work, more detailed studies such as LPS assay and

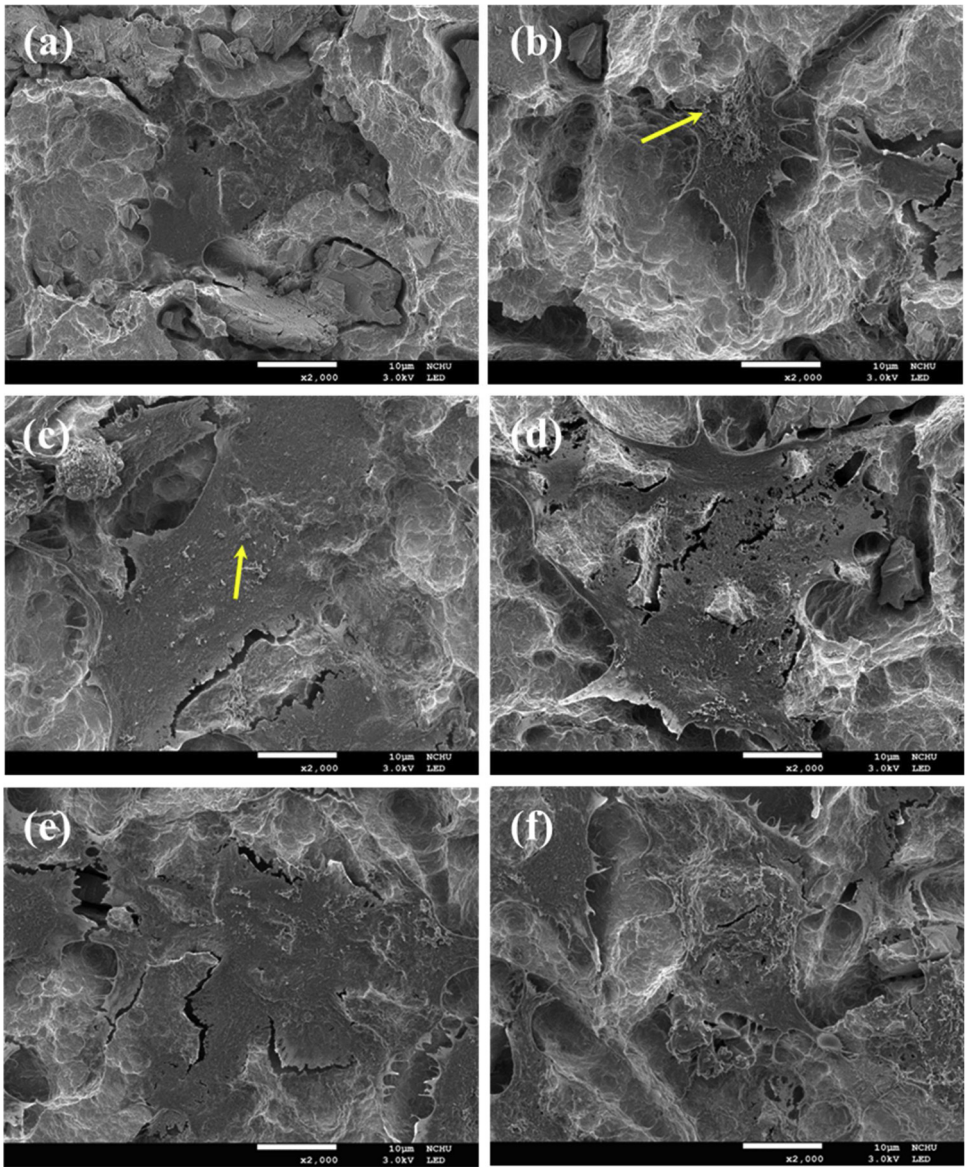

Fig. 6. SEM images of MG63 cell after 6 h of culture on (a) the uncontaminated Ti surface and *A. actinomycetcmcomitans*-contaminated surfaces treated by (b) 200, (c) 250, (d) 300, (e) 350, and (f) 400 μg/mL MB-aPDT. The arrows indicated the presence of bacteria.

cell functions would be crucial for understanding the roles of MB-aPDT. Unsurprisingly, a considerably high LPS amount remained on the contaminated surface. Conversely, a significant reduction of LPS from *A. actinomycetemcomitans* was detected after various MB-aPDT treatments. Moreover, a clear reverse correlation between the used MB concentration and residual LPS amount could be seen. Of note, the absorbance on the disinfected Ti alloy surface using 400 μg/mL MB-aPDT was comparable to the detection limit of the endotoxin assay kit.

The implant materials should support cell and tissue growth, thereby enhancing bone defect regeneration. The presence of bacteria may complicate the process of bone tissue integration, possibly conducting to a compromise between biofilm growth and osseointegration [54] or even failing to the occurrence of osseointegration [55]. Gristina [56] interpreted that the fate of a biomaterial implant was regarded as a race between microorganism adhesion and biofilm growth on an implant surface vs. tissue integration. Subbiahdoss et al. [57] also reported that the outcome of the race for the implant surface between bacteria and tissue cells depended on the number of bacteria present before osteoblast seeding. After removal of bacterial adhesion or biofilms, host cell reattach and growth should be evaluated to ascertain the success of the therapy. A search of the literature showed few reports that addressed the effects of the aPDT treatment on osteoblastic functions, when the cells cultured on disinfected implant surfaces [40]. Eick et al. [40] found that the cell attachment of SLA Ti implant after biofilm removal by aPDT was comparable to the control without bacteria. In this regard, the attachment, proliferation, differentiation, and mineralization of MG63 cells were examined. It was concerned about whether osteoblast functions can be enhanced on the surfaces of the contaminated implants treated by MB-aPDT.

Cell behavior such as attachment and proliferation represent the initial phase of cell–material communication that subsequently effect differentiation and mineralization [58]. The results of the current study clearly revealed that aPDT with the low MB concentration such as 200 μg/mL affected adversely MG63 cell attachment and proliferation. This can be explained by fact that this low MB concentration in MB-aPDT had a greater bacterial colony and residual LPS on the disinfected surface than the high concentration use of MB-aPDT. In fact, the slow cell growth is possibly because of poisoning by residual LPS amount on the disinfected surface. According to the literature [40], adhesion of host cells is inversely related to the remained bacterial counts on the

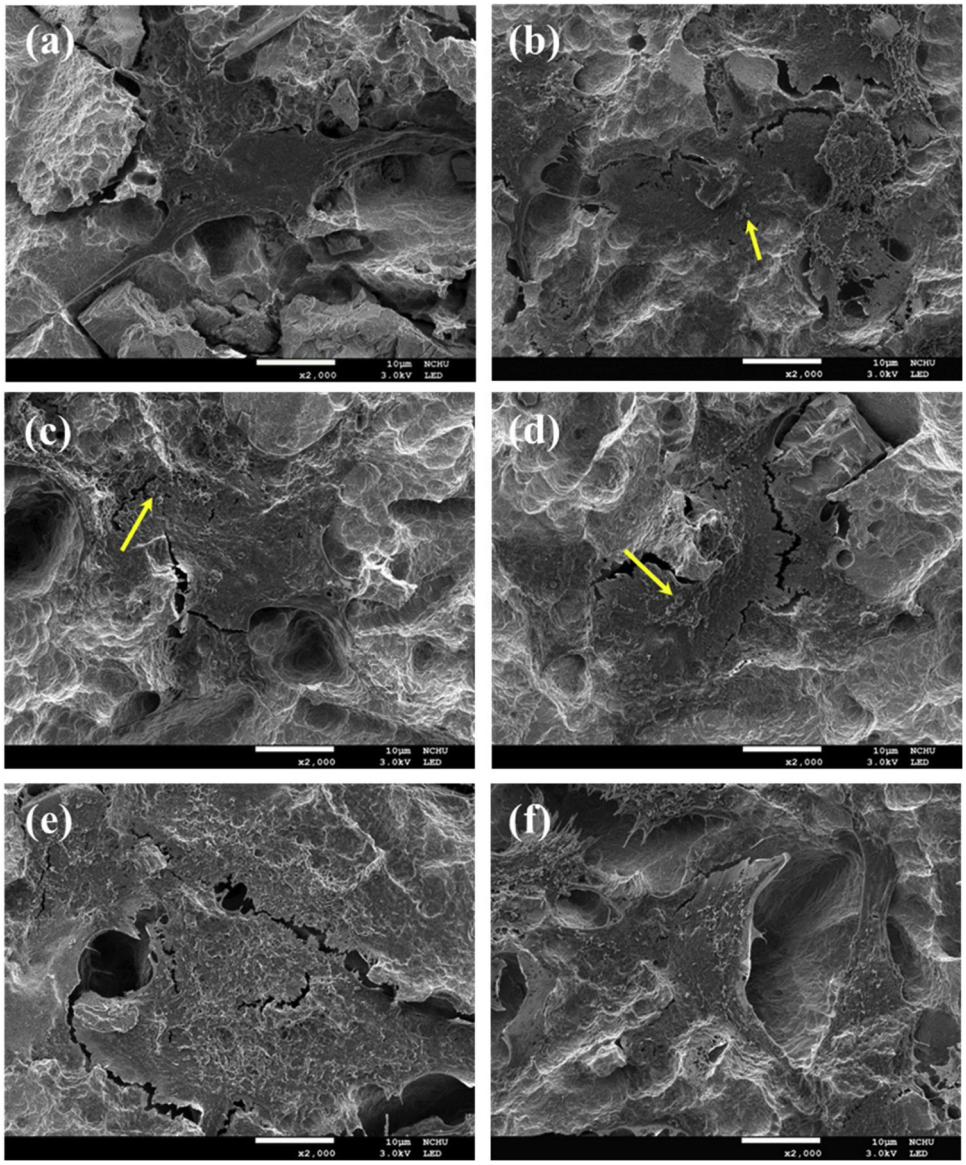

Fig. 7. SEM images of MG63 cell after 6 h of culture cultured on (a) the uncontaminated Ti surface and *S. mutants*-contaminated surfaces treated by (b) 200, (c) 250, (d) 300, (e) 350, and (f) 400 μg/mL MB-aPDT. The arrows indicated the presence of bacteria.

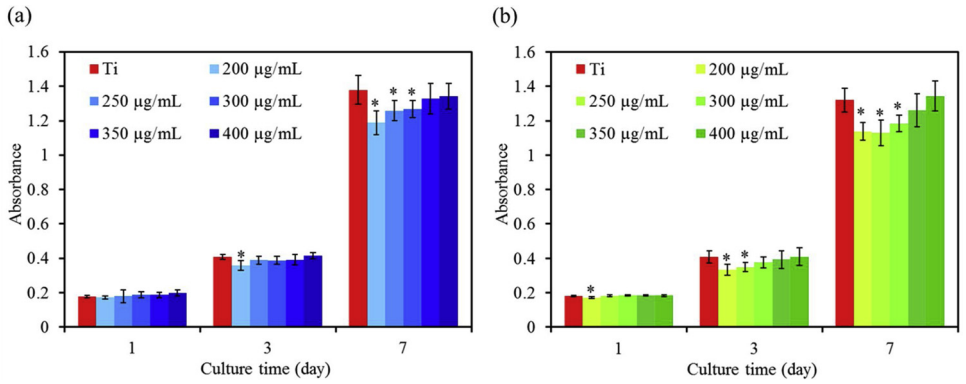

Fig. 8. Proliferation assay of MG63 cells cultured on the (a) *A. actinomycetcmcomitans*-contaminated and (b) *S. mutants*-contaminated surfaces for 1, 3, and 7 days of culture after various MB-aPDT treatments. An asterisk (*) shows the significant difference ($p < 0.05$) from the uncontaminated Ti control.

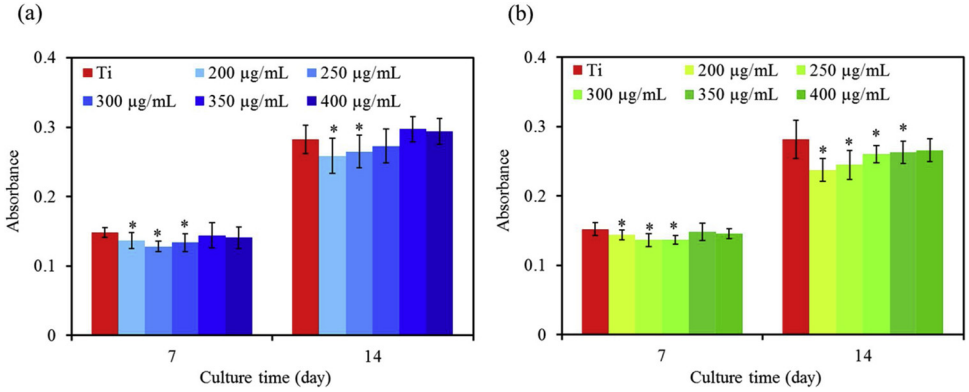

Fig. 9. ALP assay on MG63 cells cultured on the (a) *A. actinomycetcmcomitans*-contaminated and (b) *S. mutants*-contaminated surfaces for 7 and 14 days of culture after various MB-aPDT treatments. An asterisk (*) shows the significant difference ($p < 0.05$) from the uncontaminated Ti control.

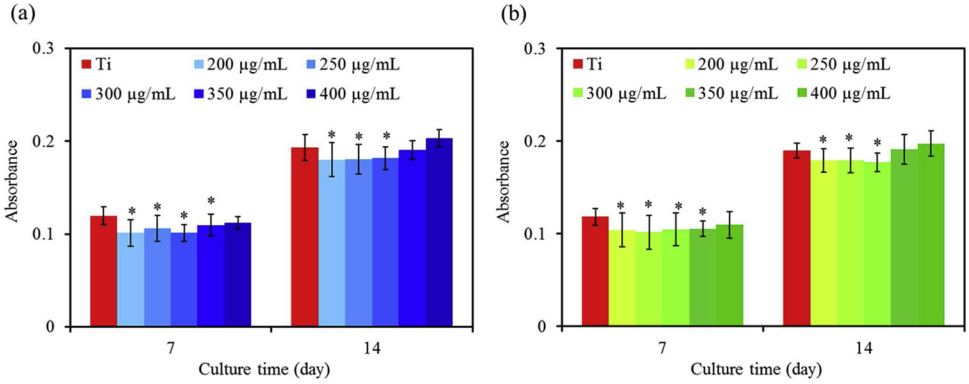

Fig. 10. Quantification of calcium mineral deposits of MG63 cells cultured on the (a) *A. actinomycetcmcomitans*-contaminated and (b) *S. mutants*-contaminated surfaces for 7 and 14 days of culture after various MB-aPDT treatments. An asterisk (*) shows the significant difference ($p < 0.05$) from the uncontaminated Ti control.

SLA surfaces. The LPS remnants interfered with osteoblast [11] and periodontal ligament fibroblasts [59]. In addition, LPS is shown to cause reduction of cell orientation [60].

Osteoblast differentiation is generally accompanied by ALP expression and in vitro mineralization [61]. In this study cell differentiation studies, like cell proliferation assay results, showed a similar trend in osteoblast response to the disinfected samples by the concentration use of MB-aPDT. MG63 cells displayed significantly increased ALP and calcium deposit levels with increasing culture time. ALP is produced in high levels during the bone formation phase [58]. The cells producing a mineralized matrix and nodules can represent the re-osseointegration ability of the disinfected implants. The results of osteogenesis-related analyses consistently indicated significant higher ALP and calcium content in the cells cultured on the 400 μg/mL MB-aPDT group than those on the other low concentration groups, which was comparable to the uncontaminated Ti implants. Thus, even if the decontamination was not fully achieved, the in vitro cell culture revealed comparable amounts of osteoblast functions, such as proliferation, differentiation, and mineralization, to the uncontaminated control. This can be because the great amounts of osteoblastic cells were seeded onto the relatively few biofilms-containing implant surfaces, and the cells could coexist with few bacteria and grow well. Finally, the decrease in the osteogenesis-related expression with the increasing culture time was not found. Moreover, the less LPS remaining on the implant surfaces would be another factor [28]. On the other hand, Nuernberg et al. [62] reported that aPDT can act over bone repair by accelerating the healing process though low-level laser photobiomodulation. Of note, LLLT on human distracted mandibles might increase the quality and quantity of bone and shorten the consolidation period [63].

The results of this in vitro study demonstrated that it is possible to significantly reduce biofilm-associated bacterial growth and to improve the osseointegration on the contaminated implant surfaces by means of MB-aPDT. Thus, taking the compromise between antibacterial efficacy and osteogenic activity into account, we may ensure that the present 400 μg/mL MB-aPDT treatment might be suitable for use in peri-implantitis therapy. Within the limits of this in vitro model using SLA disc samples rather than commercially screw-shaped dental implants, further investigations are needed to conduct the optimization of treatment protocols, such as laser fluency and the residence time of the photosensitizer, on the commercial dental implants for achieving superior bactericidal efficacy and enhanced osteogenic activity in the management of peri-implantitis.

5. Conclusion

This study supported the hypothesis of the concentration-dependent eradication efficacy of the MB-aPDT treatment against *A. actinomycetemcomitans* and *S. mutans* on the surface of SLA Ti alloys. The use of a high MB concentration in aPDT enhanced osteoblast functions, including attachment, proliferation, differentiation, and mineralization cultured on the biofilm-contaminated surfaces, which were comparable to those on the uncontaminated control. The aPDT treatment with 400 μg/mL MB photosensitizer was a promising alternative method for peri-implantitis.

References

[1] N.U. Zitzmann, T. Berglundh, Definition and prevalence of peri-implant diseases, J. Clin. Periodontol. 35 (2008) 286–291.

[2] L.J. Tavares, A.C. Pavarina, C.E. Vergani, E.D. de Avila, The impact of antimicrobial photodynamic therapy on peri-implant disease: what mechanisms are involved in this novel treatment? Photodiagn. Photodyn. Ther. 17 (2017) 236–244.
[3] A. Mellado-Valero, P. Buitrago-Vera, M.F. Solá-Ruiz, J.C. Ferrer-García, Decontamination of dental implant surface in peri-implantitis treatment: a literature review, Med. Oral Patol. Oral Cir. Bucal 18 (2013) e869–e876.
[4] N.S. Soukos, J.M. Goodson, Photodynamic therapy in the control of oral biofilms, Periodontology 55 (2011) (2000) 143–166.
[5] J. Marotti, P. Tortamano, S. Cai, M.S. Ribeiro, J.E.M. Franco, T.T. de Campos, Decontamination of dental implant surfaces by means of photodynamic therapy, Lasers Med. Sci. 28 (2013) 303–309.
[6] C.J. Chen, S.J. Ding, C.C. Chen, Effects of surface conditions of titanium dental implants on bacterial adhesion, Photomed. Laser Surg. 34 (2016) 379–388.
[7] P.S. Stewart, M.J. Franklin, Physiological heterogeneity in biofilms, Nat. Rev. Microbiol. 6 (2008) 199–210.
[8] C.J. Chen, C.C. Chen, S.J. Ding, Effectiveness of hypochlorous acid to reduce the biofilms on titanium alloy surfaces in vitro, Int. J. Mol. Sci. 17 (2016) 1161.
[9] B.S. Lee, K.S. Shih, C.H. Lai, Y. Takeuchi, Y.W. Chen, Surface property alterations and osteoblast attachment to contaminated titanium surfaces after different surface treatments: an in vitro study, Clin. Impl. Dent. Relat. Res. 20 (2018) 583–591.
[10] C.A. Fux, J.W. Costerton, P.S. Stewart, P. Stoodley, Survival strategies of infectious biofilms, Trends Microbiol. 13 (2005) 34–40.
[11] S. Kotsovilis, I.K. Karoussis, M. Trianti, I. Fourmousis, Therapy of peri-implantitis: a systematic review, J. Clin. Periodontol. 35 (2008) 621–629.
[12] N. Tomomatsu, K. Aoki, N. Alles, N.S. Soysa, A. Hussain, H. Nakachi, S. Kita, H. Shimokawa, K. Ohya, T. Amagasa, LPS-induced inhibition of osteogenesis is TNF-α dependent in a murine tooth extraction model, J. Bone Miner. Res. 24 (2009) 1770–1781.
[13] T. Maisch, J. Baier, B. Franz, M. Maier, M. Landthaler, R.M. Szeimies, W. Bäumler, The role of singlet oxygen and oxygen concentration in photodynamic inactivation of bacteria, Proc. Natl. Acad. Sci. U. S. A. 104 (2007) 7223–7228.
[14] J.P. Tardivo, A.D. Giglio, C.S. de Oliveira, D.S. Gabrielli, H.C. Junqueira, D.B. Tada, D. Severino, R.F. Turchiello, M.S. Baptista, Methylene blue in photodynamic therapy: from basic mechanisms to clinical applications, Photodiagn. Photodyn. Ther. 2 (2005) 175–191.
[15] M. Giannelli, G. Landini, F. Materassi, F. Chellini, A. Antonelli, A. Tani, D. Nosi, S. Zecchi-Orlandini, G.M. Rossolini, D. Bani, Effects of photodynamic laser and violet-blue led irradiation on *Staphylococcus aureus* biofilm and *Escherichia coli* lipopolysaccharide attached to moderately rough titanium surface: in vitro study, Lasers Med. Sci. 32 (2017) 857–864.
[16] T.C. Huang, C.J. Chen, S.J. Ding, C.C. Chen, Antimicrobial efficacy of methylene blue-mediated photodynamic therapy on titanium alloy surfaces in vitro, Photodiagn. Photodyn. Ther. 25 (2019) 7–16.
[17] A. Widodo, D. Spratt, V. Sousa, A. Petrie, N. Donos, An in vitro study on disinfection of titanium surfaces, Clin. Oral. Impl. Res. 27 (2016) 1227–1232.
[18] G. Sivaramakrishnan, K. Sridharan, Photodynamic therapy for the treatment of peri-implant diseases: a network meta-analysis of randomized controlled trials, Photodiagn. Photodyn. Ther. 21 (2018) 1–9.
[19] K. Yuan, Y.J. Chan, K.C. Kung, T.M. Lee, Comparison of osseointegration on various implant surfaces after bacterial contamination and cleaning: a rabbit study, Int. J. Oral Maxillofac. Impl. 29 (2014) 32–40.
[20] T. Berglundh, L. Persson, B. Klinge, A systematic review of the incidence of biological and technical complications in implant dentistry reported in prospective longitudinal studies of at least 5 years, J. Clin. Periodontol. 29 (2002) 197–212.
[21] A. Mombelli, Microbiology and antimicrobial therapy of peri-implantitis, Periodontology 28 (2002) (2000) 177–189.
[22] F. Chellini, M. Giannelli, A. Tani, L. Ballerini, L. Vallone, D. Nosi, S. Zecchi-Orlandini, C. Sassoli, Mesenchymal stromal cell and osteoblast responses to oxidized titanium surfaces pre-treated with λ = 808 nm GaAlAs diode laser or chlorhexidine: in vitro study, Lasers Med. Sci. 32 (2017) 1309–1320.
[23] F. Schwarz, A. Sculean, G. Romanos, M. Herten, N. Horn, W. Scherbaum, J. Beckeret, Influence of different treatment approaches on the removal of early plaque biofilms and the viability of SAOS2 osteoblasts grown on titanium implants, Clin. Oral Investig. 9 (2005) 111–117.
[24] M.H. Zablotsky, D.L. Diedrich, R.M. Meffert, Detoxification of endotoxin-contaminated titanium and hydroxyapatite-coated surfaces utilizing various chemotherapeutic and mechanical modalities, Implant Dent. 1 (1992) 154–158.
[25] T. Mang, S. Rogers, D. Keinan, K. Honma, R. Baier, Antimicrobial photodynamic therapy (aPDT) induction of biofilm matrix architectural and bioadhesive modifications, Photodiagn. Photodyn. Ther. 13 (2016) 22–28.
[26] C. Hegedűs, C.C. Ho, A. Csík, S. Biri, S.J. Ding, Enhanced physicochemical and biological properties of ion-implanted titanium using electron cyclotron resonance ion sources, Materials 9 (2016) 25.
[27] C.K. Wei, S.J. Ding, Dual-functional bone implants with antibacterial ability and osteogenic activity, J. Mater. Chem. B 5 (2017) 1943–1953.
[28] M. Kreisler, W. Kohnen, A.B. Christoffers, H. Götz, B. Jansen, H. Duschner, B. d'Hoedt, In vitro evaluation of the biocompatibility of contaminated implant surfaces treated with an Er:YAG laser and an air powder system, Clin. Oral Impl. Res. 16 (2005) 36–43.
[29] J. Green, A. Weiss, A. Stern, Lasers and radiofrequency devices in dentistry, Dent. Clin. North Am. 55 (2011) 585–597.
[30] Ricardo R.A. Hayek, Ney S. Araújo, Marco A. Gioso, Jonathan Ferreira, Carlos A. Baptista-Sobrinho, Aécio M. Yamada Jr., Martha S. Ribeiro, Comparative study between the effects of photodynamic therapy and conventional therapy on microbial reduction in ligature-induced peri-implantitis in dogs, J. Periodontol. 76 (2005) 1275–1281.
[31] R.R. Poppi, A.L.D. Silva, R.S. Nacer, R.P. Vieira, L.V.F. Oliveira, N.S. Faria Júnior, P.T.C. Carvalho, Evaluation of the osteogenic effect of low-level laser therapy (808 nm and 660 nm) on bone defects induced in the femurs of female rats submitted to ovariectomy, Lasers Med. Sci. 26 (2011) 515–522.
[32] R. Hübler, E. Blando, L. Gaião, P.E. Kreisner, L.K. Post, C.B. Xavier, M.G. Oliveira, Effects of low-level laser therapy on bone formed after distraction osteogenesis, Lasers Med. Sci. 25 (2010) 213–219.
[33] K. Mizutani, A. Aoki, D. Coluzzi, R. Yukna, C.Y. Wang, V. Pavlic, Y. Izumi, Lasers in minimally invasive periodontal and peri-implant therapy, Periodontology 71 (2016) (2000) 185–212.
[34] S.A. Al-Maweri, F. Javed, B. Kalakonda, N.A. AlAizari, W. Al-Soneidar, A. Al-Akwa, Efficacy of low level laser therapy in the treatment of burning mouth syndrome: a systematic review, Photodiagn. Photodyn. Ther. 17 (2017) 188–193.
[35] A. Crous, H. Abrahamse, Low-intensity laser irradiation at 636 nm induces increased viability and proliferation in isolated lung cancer stem cells, Photomed. Laser Surg. 34 (2016) 525–532.
[36] A. Castilho-Fernandes, T.G. Lopes, F.U. Ferreira, N. Rezende, V.F. Silva, F.L. Primo, A.M. Fontes, A. Ribeiro-Silva, A.C. Tedesco, Adipogenic differentiation of murine bone marrow mesenchymal stem cells induced by visible light via photo-induced biomodulation, Photodiagn. Photodyn. Ther. 25 (2019) 119–127.
[37] V.G. Garcia, E.C. Gualberto Júniora, E. Ervolino, M.J.H. Nagata, J.M. de Almeida, L.H. Theodoro, aPDT for periodontitis treatment in ovariectomized rats under systemic nicotine, Photodiagn. Photodyn. Ther. 22 (2018) 70–78.
[38] J.M. de Almeida, L.H. Theodoro, A. Francisco Bosco, M.J.H. Nagata, M. Oshiiwa, V.G. Garcia, In vivo effect of photodynamic therapy on periodontal bone loss in dental furcations, J. Periodontol. 79 (2008) 1081–1088.
[39] K. Subramani, D. Wismeijer, Decontamination of titanium implant surface and re-osseointegration to treat peri-implantitis: a literature review, Int. J. Oral Maxillofac. Impl. 27 (2012) 1043–1054.
[40] S. Eick, I. Meier, F. Spoerlé, P. Bender, A. Aoki, Y. Izumi, G.E. Salvi, A. Sculean, In vitro-activity of Er:YAG laser in comparison with other treatment modalities on biofilm ablation from implant and tooth surfaces, PLoS One 12 (2017) e0171086.
[41] J. Chen, T.C. Cesario, P.M. Rentzepis, Effect of pH on methylene blue transient states and kinetics and bacteria photoinactivation, J. Phys. Chem. A 115 (2011) 2702–2707.
[42] R.J. Watts, V.D. Adams, E. Middlebrooks, Effect of pH on the indirect photolysis treatment of three refractory herbicides, J. Chemos. 17 (1988) 2083–2091.
[43] B. Leblebicioglu, J.S. Lim, A.C. Cario, F.M. Beck, J.D. Walters, pH changes observed in the inflamed gingival crevice modulate human polymorphonuclear leukocyte activation in vitro, J. Periodontol. 68 (1996) 472–477.
[44] A. Lardner, The effects of extracellular pH on immune function, J. Leukocyte Biol. 69 (2001) 522–530.
[45] I. Abrahamsson, T. Berglundh, E. Linder, N.P. Lang, J. Lindhe, Early bone formation adjacent to rough and turned endosseous implant surfaces. An experimental study in the dog, Clin. Oral Impl. Res. 15 (2004) 381–392.
[46] M. Klausen, A. Heydorn, P. Ragas, L. Lambertsen, A. Aaes-Jørgensen, S. Molin, T. Tolker-Nielsen, Biofilm formation by *Pseudomonas aeruginosa* wild type, flagella and type IV pili mutants, Mol. Microbiol. 48 (2003) 1511–1524.
[47] L.E. DeForge, K.L. Billeci, S.M. Kramer, Effect of IFN-γ on the killing of *S. Aureus* in human whole blood: assessment of bacterial viability by CFU determination and by a new method using alamarBlue, J. Immunol. Methods 245 (2000) 79–89.
[48] M. Wainwright, K.B. Crossley, Methylene blue: a therapeutic dye for all seasons? J. Chemother. 14 (2002) 431–443.
[49] D.P. Aureliano, J.A.L. Lindoso, S.R.C. Soares, C.F.H. Takakura, T.M. Pereira, M.S. Ribeiro, Cell death mechanisms in *Leishmania amazonensis* triggered by methylene blue-mediated antiparasitic photodynamic therapy, Photodiagn. Photodyn. Ther. 23 (2018) 1–8.
[50] M.N. Usacheva, M.C. Teichert, M.A. Biel, The role of the methylene blue and toluidine blue monomers and dimers in the photoinactivation of bacteria, J. Photochem. Photobiol. B 71 (2003) 87–98.
[51] C.R. Fontana, A.D. Abernethy, S. Som, K. Ruggiero, S. Doucette, R.C. Marcantonio, C.I. Boussios, R. Kent, J.M. Goodson, A.C. Tanner, N.S. Soukos, The antibacterial effect of photodynamic therapy in dental plaque-derived biofilms, J. Periodontal. Res. 44 (2009) 751–759.
[52] M. Longo, V.G. Garcia, E. Ervolino, M.L.F. Alves, C. Duque, M. Wainwright, L.H. Theodoro, Multiple aPDT sessions on periodontitis in rats treated with chemotherapy: histomorphometrical, immunohistochemical, immunological and microbiological analyses, Photodiagn. Photodyn. Ther. 25 (2019) 92–102.
[53] T. Ohsumi, S. Takenaka, R. Wakamatsu, Y. Sakaue, N. Narisawa, H. Senpuku, H. Ohshima, Y. Terao, T. Okiji, Residual structure of Streptococcus mutans biofilm following complete disinfection favors secondary bacterial adhesion and biofilm redevelopment, PLoS One 10 (2015) e0116647.
[54] J. Geurts, J.J. Chris Arts, G.H.I.M. Walenkamp, Bone graft substitutes in active or suspected infection. Contra-indicated or not? Int. J. Care Injured. 42 (2011) S82–S86.
[55] L.G. Persson, I. Ericsson, T. Berglundh, J. Lindhe, Osseintegration following treatment of peri-implantitis and replacement of implant components. An experimental study in the dog, J. Clin. Periodontol. 28 (2001) 258–263.
[56] A.G. Gristina, Biomaterial-centered infection: microbial adhesion versus tissue integration, Science 237 (1987) 1588–1595.
[57] G. Subbiahdoss, R. Kuijer, D.W. Grijpma, H.C. van der Mei, H.J. Busscher, Microbial biofilm growth vs. tissue integration: "The race for the surface" experimentally studied, Acta Biomater. 5 (2009) 1399–1404.
[58] S.J. Ding, Y.H. Chu, D.Y. Wang, Enhanced properties of novel zirconia-based osteoimplant systems, Appl. Mater. Today 9 (2017) 622–632.
[59] T.T. Hägi, S. Klemensberger, R. Bereiter, S. Nietzsche, R. Cosgarea, S. Flury,

A. Lussi, A. Sculean, S. Eick, A biofilm pocket model to evaluate different non-surgical periodontal treatment modalities in terms of biofilm removal and re-formation, surface alterations and attachment of periodontal ligament fibroblasts, PLoS One 10 (2015) e0131056.

[60] F.J. Hughes, F.C. Smales, Attachment and orientation of human periodontal ligament fibroblasts to lipopolysaccharide-coated and pathologically altered cementum in vitro, Eur. J. Prosthodont. Restor. Dent. 1 (1992) 63–68.

[61] I.T. Wu, T.Y. Chiang, C.C. Chen, Y.C. Chen, S.J. Ding, Dopant-dependent tailoring of physicochemical and biological properties of calcium silicate bone cements, Biomed. Mater. Eng. 29 (2018) 773–785.

[62] M.A.A. Nuernberg, D.M.J. Miessi, C.A. Ivanaga, M.B. Olivo, E. Ervolino, V.G. Garcia, M. Wainwright, L.H. Theodoro, Influence of antimicrobial photodynamic therapy as an adjunctive to scaling and root planing on alveolar bone loss: a systematic review and metaanalysis of animal studies, Photodiagn. Photodyn. Ther. 25 (2019) 354–363.

[63] A.Z. Abd-Elaal, H.A. El-Mekawii, A.M. Saafan, L.A. El Gawad, Y.M. El-Hawary, M.A. Abdelrazik, Evaluation of the effect of low-level diode laser therapy applied during the bone consolidation period following mandibular distraction osteogenesis in the human, Int. J. Oral Maxillofac. Surg. 44 (2015) 989–997.